Advances in Science and Technology Research Journal

Advances in Science and Technology Research Journal, 2025, 19(11), 221–229
https://doi.org/10.12913/22998624/209288
ISSN 2299-8624, License CC-BY 4.0

Received: 2025.06.23
Accepted: 2025.09.15
Published: 2025.10.01

Analysis of the effect of scandium halide on energy and current transfer in unbalanced plasma layers near the cathode surface in arc discharge

Rafid Abbas Ali[1*], Faten Sajet Mater[1]

[1] Department of physics, College science, Mustansiriyah University, Baghdad, Iraq
* Corresponding author's e-mail: rafidphy_1972@uomustansiriyah.edu.iq

ABSTRACT

Halide addition to xenon plasma enhances performance in electric discharge systems and high-intensity light sources, making it a practical strategy for various applications. This study examines the impact of adding scandium halide ScI to xenon plasma, using two concentrations (Sc 0.1% and 5%) and a 0.1% iodine content. The investigation was conducted under two discharge voltages to assess changes in cathode-plasma interaction, energy transport mechanisms, and current behavior. The research focuses on two aspects: energy transport to the cathode, including total energy flux, ion energy, fast electron energy, and thermionic emission losses, and the behavior of various current densities at the cathode surface, including changes in cathode sheath voltage and effective work function. The study found that at a low concentration of Sc 0.1%, the discharge characteristics of xenon remain similar to pure xenon, indicating minimal disruption to the plasma environment. However, at Sc 5%, energy transfer efficiency improved significantly, with a 30% increase in total energy flux due to enhanced ionization, reduced thermionic energy loss, and improved energy transport. The analysis of current density showed that components increase with cathode surface temperature, with thermionic electron emission becoming the dominant current mechanism at higher temperatures. This transition occurred more rapidly at 25 V and with higher ScI concentration. The intersection point between j_{em} and total current shifted to lower temperatures. The cathode sheath voltage decreased with improved electron emission, indicating a shift towards a space-charge limited regime. ΔA and floating potential exhibited temperature-dependent behavior. The study demonstrates that the addition of scandium iodide at a Sc 5% concentration, even with a low iodine content, significantly enhances plasma performance by increasing energy flux, enhancing current transfer efficiency, and reducing cathode energy losses.

Keywords: arc discharge, voltage barrier, Schottky correction, electron temperature, voltage of the ionization layers near the cathode, current flux density.

INTRODUCTION

Non-linear cathode surface heating significantly contributes to current generation in high-pressure arc discharges [1, 2]. The current transfer model in electric arc discharges is based on solving the thermal conductivity equation of the cathode electrode, focusing on the transfer of energy density after plasma generation to the cathode's surface, resulting in a drop in potential of unbalanced layers close to the cathode's surface [3, 4], but this process leads to the occurrence of a state of instability in the current transfer [5]. The concept of arc discharge ignition is of great practical importance for high currents in high atmospheric pressure gases [6, 7], there are several hypotheses that regulate the transfer of current to the cathode surface [8, 9] By understanding the mechanism of interaction of the plasma layers close to the cathode surface in the arc discharge plasma [10, 11]. There are several studies on this subject about the process of transferring excited electrons with ionic charges to the surface of the cathode, this results in the surface's electron emission [12–15]. These studies demonstrated the actual mechanism of current transfer to the cathode

surface, as the transfer process was very short and the ion current had a direct effect on keeping the cathode hot. These studies played an important role in developing the stability of current emission and a major role in using these developments in applications through the production of high-efficiency, long-life light lamps [16]. In this research, a model of the interaction of plasma layers near the cathode surface was used, based on a xenon plasma with the addition of metal halide (XH) in the form of scandium iodine, at different concentrations concentrations (0.1% and 5%) with a fixed iodine content of 0.1% to investigate the effect of these concentrations on the plasma current density, the current density of electrons, ions, and electrons emission from the cathode surface, using a tungsten cathode with a radius of 0.001 m and a distance between the electrodes of 0.01 m, at a pressure of 1 bar. The thermionic emission current from the cathode surface was determined using the Richardson-Dushman equation. The simulation was run using an applied voltage range of 13 V to 15 V and a cathode surface temperature range of 3000 K to 4400 K. Quantitative results were obtained illustrating the relationships between $j, j_e, j_{em}, j_i, q, q_e, q_{em}, q_i, T_w, T_e, \Delta A, U_i, I$ as shown in Figure 1.

MODEL OF THE INTERACTION OF PLASMA LAYERS NEAR THE SURFACE OF THE CATHODE

The modeling of layers near the cathode surface in high-pressure arc discharge involves two parts: the cathode modeling part and the full arc modeling part. This case has been developed previously and in an excellent manner [17]. The non-linear thermal cathode surface model as shown in Figure 2 is determined by assuming that the cathode used has a conductivity of k, a specific heat of C, and a density of ρ, as a functions of the temperature T, where $p = p(T)$, $k = k(T)$ and $C_p = C_p(T)$.

The Figure 2 illustrates a cathode with two parts, where plasma particles should touch one part to increase the cathode's temperature and generate current.. The other part of the cathode is supposed to touch the gas, Here, the cathode can lose energy through radiation or exchange heat with the gas. In both parts, the main role is the temperature of the cathode surface [19]. The energy flow function $q = q(Tw.\ U)$ describes the heating of the cathode surface due to current flow from nearby layers for all $T_w \geq T_c$ values, where T_w is the cathode surface temperature and the cathode base temperature respectively.

This function describes the direct relationship between the arc discharge and the gas for the two cathode parts. Arc plasma generates energy in current accumulation near cathode surface, with temperature controlling current and accompanied by voltage drop U in layers near cathode surface. As is known, the generated current and energy flow are direct functions of T_w and voltage U [20]. The cathode surface's contact with the gas causes a drop in temperature, making the energy flow function independent of voltage U. This function describes energy losses due to radiation or heat exchange between the cathode and the gas. Another function, $j = j(T_w, U)$, describes the transfer of current from layers close to the cathode surface when T_w is high and $T_w \geq T_c$. However, in the case of a decrease in the current values, this function becomes ineffective [21].

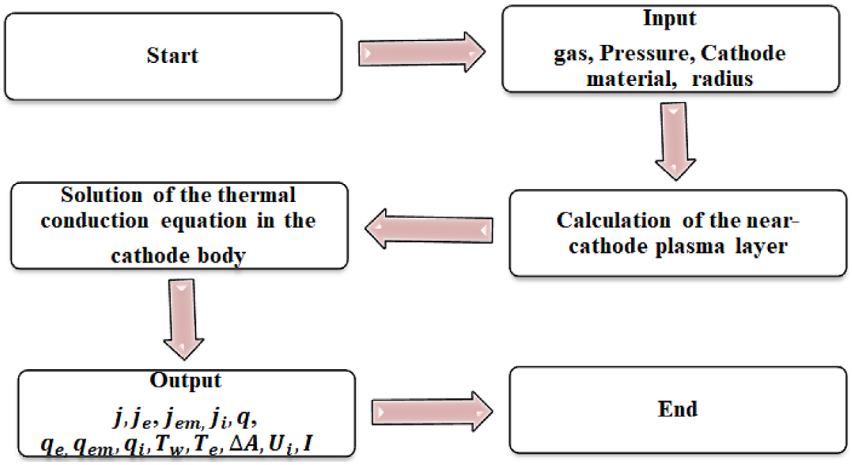

Figure 1. Flow chart for the near-cathode plasma layers simulation

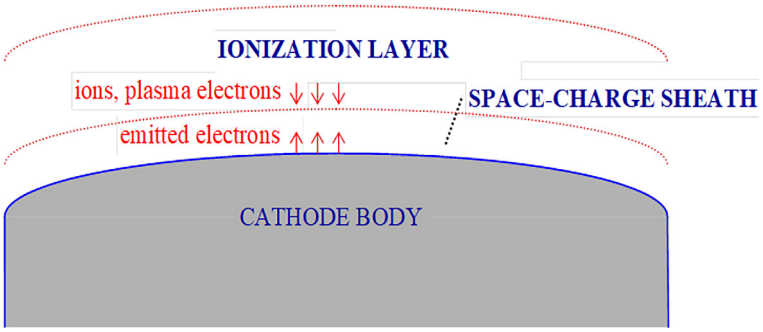

Figure 2. The near-cathode layer schematic [18]

The temperature distribution on the cathode surface is described by the thermal conductivity equation. [18]:

$$\rho(T)C_p(T)\frac{\partial T}{\partial t} = \nabla.[k(T)\nabla T] \quad (1)$$

$$\nabla.k\nabla T = 0 \quad (2)$$

Equation 1 can be solved by specifying some conditions [22]:

$$T = T_c, k\frac{\partial T}{\partial n} = q(T_W, U) \quad (3)$$

where: k represents the thermal conductivity and T_c is the cathode base temperature, which is a function of the energy flux density.

Solving Equation 1 will provide a clear understanding of temperature distribution, current density, and energy flow to the cathode surface, as the transfer of energy depends on the local surface temperature [23]. The interaction process between the plasma layers near the cathode surface and the cathode surface is determined through several conditions. The first is to give an accurate picture of how the current is transferred to the cathode surface and the relationship of the current to the cathode temperature T_W and the voltage U, which gives an accurate description of how the energy $q = q(T_W, U)$ and the current $j = j(T_W, U)$ flows from the layers to the place where the current accumulates on the surface. The second case is that the energy flow function must be approximately equal to the total plasma energy flux density q_p at high T_W and is known for all values of $T_W \geq T_C$ and explains the mutual heat transfer between the cathode and the gas at the point of contact and makes the value of the current density j equal to zero at low temperatures T_W. The last case is to solve Equation 1 [24].

The model is based on the accumulation of charges near the cathode, which is the region from which energy flows. The cathode temperature rises in this region due to the production of ions, which are rapidly transported by the electric field to the cathode along with electrons [25]. The plasma energy flowing to the cathode surface can be calculated using the following relationships [26]:

$$q_p = q_e + q_i - q_{em} \quad (4)$$

$$q_i = j_i\left[Z_eU_D + E - ZA_{eff} + k\left(2T_h + \frac{ZT_e}{2} - 2T_w\right)\right] \quad (5)$$

$$q_e = j_e\left(2kT_e + A_{eff}\right) \quad (6)$$

$$q_{em} = j_{em}\left(2kT_w + A_{eff}\right) \quad (7)$$

The energy densities of ions and electrons from plasma layers near the cathode surface are represented by q_i and q_e, while q_{em} represents the energy flux density emitted due to thermionic emission. The electric current densities of ions and electrons moving to the cathode surface and emitted from the cathode surface are represented by $j_i = ZeJ$, $j_e = eJ_e$, $j_{em} = eJ_{em}$, Where the flux of ions, flux of electrons, and flux of electrons emitted from the cathode surface are denoted by J_i, J_e, and J_{em} respectively. While T_h, T_e represents the temperature of heavy particles and electrons. The ionization energy rate in the layers near the cathode surface is represented by Z, which represents the number of ions' charges. U_D represents the low potential inside the space charge shell and its relationship is usually inversely with the low potential in the primary shell $U_i = U - U_D$ [27] where the space charge sheath's voltage drop is denoted by U_D and A_{eff} is the effective work function [27]. Equation 5 can be rewritten as follows [27]:

$$q_i = j_i\left(z_eU_D + E - ZA_{eff}\right) + W_i + \\ + \left[j_ik\left(2T_h + \frac{ZT_e}{2}\right) - (j_i2kT_w + W_i)\right] \quad (8)$$

where: W_i is the average value of the current in the ionized layers near the cathode surface.

This equation consists of two terms, the first term from the right represents the energy of the ions flowing from the layers close to the cathode surface to the space atmosphere and the second term represents the energy of the neutral atoms in the ionization layers. The stability of the plasma discharge makes the terms of the second term (on the right) of the above equation equal and thus Equation 7 becomes:

$$q_i = j_i\left(z_e U_D + E - ZA_{eff}\right) + W_i \tag{9}$$

Through Equations 4, 6, 7 and 9 we can obtain the energy balance equation for electrons in the ionization layers:

$$j_e\left(\frac{2kT_e}{2} + U_D\right) + 3.2j\frac{kT_e}{e} + j_i E = \\ = j_{em}\left(\frac{2kT_w}{e} + U_D\right) + W_e \tag{10}$$

The total plasma current transmitted to the cathode surface is $= j_i + j_{em} - j_e$, where W_e represents the direct effect of the electric field resulting from the electric charges near the surface on the electrons. From Equations 4, 6, 7, 9 and 10, and in addition to the equation $JU_i = W_e + W_j$, we obtain:

$$q_p = jU - \frac{j}{e}\left(A_{eff} + 3.2kT_e\right) \tag{11}$$

Equation 11 explains energy transfer to the surface by comparing the energy deposited per unit area from a nearby layer to the energy transferred to the plasma through electron current [27]. Equation 11 explains the difference between electron and plasma energy, as both energies are transferred from layers near the cathode surface to the cathode surface. The net energy flux transferred to the cathode surface can be calculated using the following relationship [27]:

$$q = q_p - q_r, q_r = \varepsilon\sigma T_W^4 \tag{12}$$

From Equation 11 and Equation 12, we can obtain the equation:

$$IU = Q_c + Q_r + \frac{1}{e}\left(+A_{eff}^* + 3.2kT_e^*\right) \tag{13}$$

Equation 13 shows that the electrical power (IU) represents the sum of the power reaching the cathode base Q_c, the power radiated from the surface Q_r, and the energy near the cathode surface that is transferred by the electron current $\frac{1}{e}\left(+A_{eff}^* + 3.2kT_e^*\right)$ to the surface, where:

$$Q_c = \int qdS,\ Q_r = \int q_r dS,\ A_{eff}^* = \\ = \frac{1}{I}\int jA_{eff}dS,\ T_e^* = \frac{1}{I}\int jT_e dS \tag{14}$$

Q_c is the power transmitted from the cathode surface to the base, and Q_r is the power radiated from the cathode surface. As we noted previously, for the layers close to the cathode surface, ions reach the cathode surface through the ionization layer U_i. This region is characterized by multiple collisions, unlike the vacuum charge sheath region close to the cathode surface, as in the equation [22]:

$$j_i = n_{is} v_s \tag{15}$$

where: n_{is} represents the density of electrons or charges at the edge of the shell and $v_s v_s$ is the Bohm velocity and is given by the relationship [22]:

$$v_s = \sqrt{\frac{k(T_h + T_e)}{m_i}} \tag{16}$$

where: m_i is the mass of the ion.

The relationship between electron flux and their arrival at the cathode surface after crossing the potential barrier is given [22]:

$$j_e = \frac{1}{4} n_{is}\sqrt{\frac{8kT_e}{\pi m_e}}\ exp\left(-\frac{eU_D}{kT_e}\right) \tag{17}$$

The flow of electrons creates an electric field on the cathode's surface, causing heat emission from the cathode. This emission is determined by the Richardson-Dushman equation [28]:

$$J_{em} = CT^2 e^{-\frac{A-\Delta A}{K_B T}} \tag{18}$$

where: C, K_B, A, ΔA are the Richardson constant, Boltzmann constant, metal work function and Schottky correction respectively.

This field can be calculated using the Boltzmann equation, which describes ion movement, and the solution of the Poisson equation, as in the relationship [27]:

$$E_w = \sqrt{\frac{2n_{is}kT_h}{\epsilon_0}}\left[\frac{v_+^3 - v_-^3}{6U_i^3} - \frac{4}{3} - 2\beta + \right. \\ \left. + \beta exp\left(-\frac{eU_D}{kT}\right)\right]^{1/2} \tag{19}$$

$$U_i = \sqrt{\frac{kT_h}{m_i}},\ \beta = \frac{T_e}{T_h},\ v_\pm = \left[(v_s \pm U_i)^2 + \frac{2eU_D}{m_i}\right]^{1/2} \tag{20}$$

The current density can be calculated using the following relationship:

$$j = e(j_i + j_{em} - j_e) \quad (21)$$

The evolution of the particle density is possible to calculate by Saha's equation where conditional bands of suitable ionization state are required on occasions:

$$\frac{n_{is}}{n_{i\infty}} = \frac{\alpha C_2\sqrt{1+\beta}}{C_2 + 2\alpha C_2\sqrt{1+\beta} + \alpha^2\sqrt{1+\beta}} \quad (22)$$

Where C_2 is a dimensionless coefficient [33] and α represents the ratio of the ionization length to the mean free path of collisions and is given by the following relation [34]:

$$\alpha = \sqrt{\frac{2}{3}\frac{C_{ia}Q_{ia}}{k_i}},\ Q_{ia} = \sqrt{\frac{8kT_h}{\pi}\left(\frac{1}{m_i} + \frac{1}{m_a}\right)} \quad (23)$$

where: Q_{ia} is the cross-sectional average of the momentum transferred due to elastic collisions between electrons and atoms, k_i is the ionization rate constant for the gas, C_{ia} is the relative velocity of the ions and atoms, and m_i and m_a are the masses of the ions and atoms. The above relationships represent a precise and comprehensive interpretation of the interactions of the plasma layers near the cathode surface as functions of T_W and U.

RESULTS

The study investigated the variation in energy flux components from plasma to cathode surface based on surface temperature for XH concentration (Sc 0.1% and 5%.) at 13 volts and 25 volts, as shown in Figures 3 and 4. Figure 3a shows that at 13 volts, pure xenon plasma shows a peak in total energy flux q_p around 3800 K, indicating an optimal balance between ion and electron heating mechanisms and radiative losses through thermionic emission. As temperature increases, q_p declines due to the dominance of q_{em}, reflecting increasing electron emission losses from the cathode surface. Ion energy contribution q_i accounts for 70–80% of q_p, primarily due to the high kinetic energy of ions accelerated through the sheath region. With temperature elevation, q_i increases until it plateaus due to enhanced ionization and energy dissipation in the ionized layer. q_e becomes increasingly significant at higher temperatures, particularly above 4000 K, due to an increase in high-energy electrons reaching the cathode. Thermionic cooling plays a crucial role at elevated temperatures, growing exponentially with temperature and surpassing ion and electron energy input, leading to a net decline in q_p. The 0.1% concentration of Sc had minimal impact, causing only slight changes in plasma parameters.

Adding Sc 5% into xenon plasma significantly improves performance, even at 13 volts as shown in Figure 3b. The total energy flux q_p increases by 15–20% due to scandium's ability to lower the effective ionization energy, facilitating more efficient energy transfer via ions and fast electrons. This leads to notable improvements in, with ion energy transport increasing by 10–15%. q_e decreases due to faster electron loss through inelastic collisions and lower average energy.

At a low discharge voltage of 13 V, the addition of Sc 0.1% exhibited minimal impact on the electron temperature T_e and ionization degree ω, with measurements remaining nearly identical to those recorded in pure xenon. When the concentration of Sc was increased to 5% at the same voltage, a significant decrease in electron temperature was noted, varying from 0.2 to 0.5 eV, accompanied by a minor reduction in the degree of ionization as shown in Figure 3a and 3b.

When voltage is raised to 25 volts, both pure and scandium-doped xenon plasmas show enhanced energy transport characteristics as shown in Figure 4. Pure xenon plasmas show higher q_p peaks between 4000 and 4200 K, due to increased energy availability from ions and fast electrons under a stronger electric field. The decline in q_p with temperature is less steep than at 13 V, due to the prolonged dominance of q_e over q_{em} at higher energies. Ion energy transport q_i increases due to vigorous ion acceleration, while electron energy transport q_e becomes more prominent, accounting for 30–40% of q_p. The plasma approaches near-complete ionization at 4200 K. Sc 0.1% had minimal impact on plasma characteristics. However, 5% Sc added to xenon plasma significantly increased total energy flux,

At a higher discharge voltage of 25 V, pure xenon's electron temperature increased significantly, reaching 5.5 eV, corresponding to a rise in ω. A low concentration of Sc 0.1% did not significantly change T_e or ω, suggesting minimal effect at dilute levels. However, with Sc 5% added at 25 V, electron temperature and ionization degree dropped significantly due to energy losses from

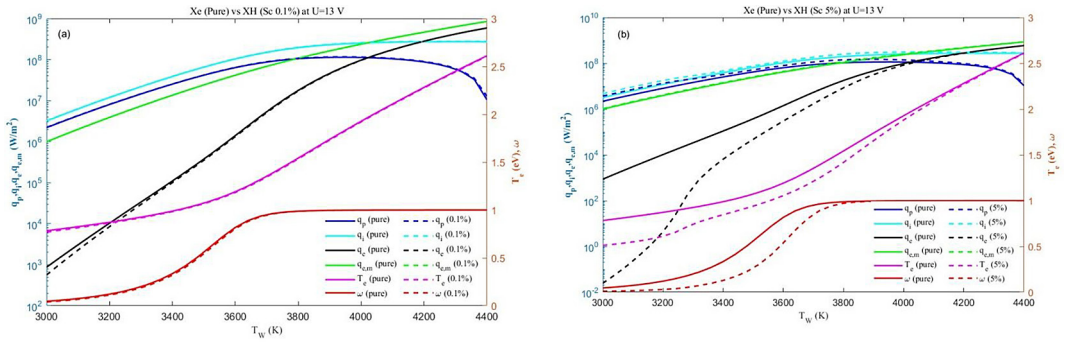

Figure 3. The energy flux components vs. the surface temperature for 13 V (a) Sc 0.1%, (b) Sc 5%

inelastic collisions between electrons and additive molecules as shown in Figure 4a and 4b.

Figure 5 and Figure 6 illustrate how the current densities (j, j_i, j_e and j_{em}) behave in relation to the cathode surface temperature T_W for both pure xenon and xenon-halide mixtures (Sc 0.1% and Sc 5%) for 13 V and for 25 V. In both voltage situations a distinct pattern is seen. All current densities typically rise when T_W rises, albeit they do so at varying rates and exhibit unique behaviors. In both gas mixes and at both voltages, the total current density j increases gradually with temperature, indicating that the cathode surface emits more charge carriers as it heats up. Although the ion current density j_i rises with Tw as well, its values are still much below the total current, suggesting that ions contribute less to the overall transmission of current than electrons.

At higher temperatures, j_{em} becomes the primary contributor to the total current j, with their values converging closely. When comparing the two voltage scenarios (13 V and 25 V), it can be seen that providing a higher voltage 25 V speeds up the transition to an electron-dominated current and produces greater values for all current densities at the same temperature. This phenomena is explained by the larger electric field at 25 V, which suppresses the relative contributions of ions and secondary plasma electrons and more efficiently pulls emitted electrons.

Current densities behavior is greatly impacted by the presence of Sc. Sc significantly increases thermionic electron emission by decreasing the cathode surface's work function. As the temperature rises and the concentration of Sc increases, this impact becomes more noticeable. There is a noticeable rise in all current densities, especially in j_{em}, when the concentration of Sc is raised to 5% (as opposed to Sc 0.1% or pure xenon).

On the other hand, especially at larger T_W values, the electron current density j_i rises exponentially with temperature. The cathode surface's increased thermionic emission is the cause of this. Je rises sharply as the temperature rises because electrons have enough thermal energy to cross the work function barrier. The change from an ion-dominated to an electron-dominated current regime is signaled by the crossover point with j_i, when j_e exceeds j_i as a result of this rise. As voltage or Sc concentration rises, this crossing becomes more noticeable. A significant change in the intersection point between j_{em} and j as well as

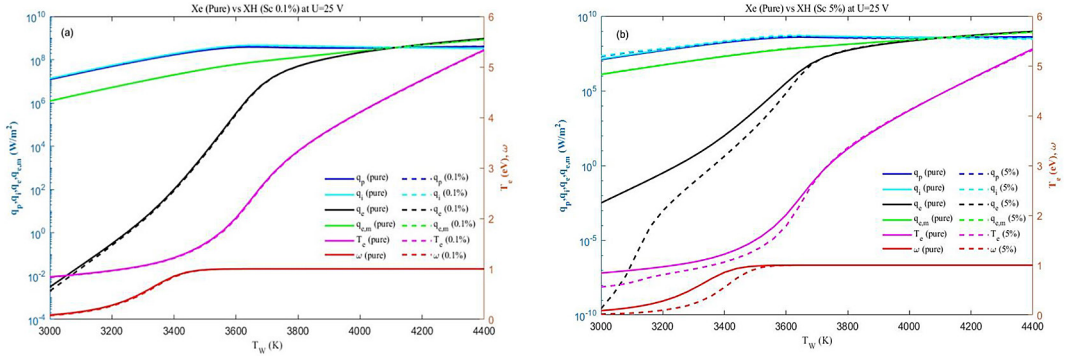

Figure 4. The energy flux components vs. the surface temperature for 25 V (a) Sc 0.1%, (b) Sc 5%

between j_e and j_i results from this enhanced j_{em} and j_e. Although this intersection happens at a higher temperature about 4100 K at 13 V with 0.1% Sc as shown in Figure 5a, it shifts to much lower temperatures as the voltage is increased (approximately 3700 K at 25 V with Sc 0.1%) as shown in Figure 6a, and it further reduces when Sc 5% concentration is used for both 13 V and 25 V.

The Schottky correction ΔA, which represents the decrease in the effective work function due to an electric field at the cathode surface, rises with the cathode surface temperature Tw. However, higher temperatures cause a redistribution of applied voltage from the sheath region to the ionization layer, lowering the electric field at the cathode surface and decreasing ΔA as shwn in Figure 5 and 6.

The peak value of ΔA in pure xenon, according to numerical calculations, is roughly 3.4 eV at T_W ≈3900 K at an arc voltage of 13 V. With Sc 0.1%, this peak drops to 3.2 eV at T_W ≈ 3700 K, and then drops to 3.0 eV at T_W ≈ 3600 K with 5% Sc. The peak values of ΔA rise generally at a higher arc voltage of 25 V because of stronger emission currents. They reach 5.5 eV in pure Xe at T_W ≈ 3700 K, 5.0 eV with Sc 0.1% at T_W ≈ 3500 K, and 4.3 eV with Sc 5% at T_W ≈3400 K. Because of the enhanced ionization that Sc offers, which enables equilibrium between electron and ion fluxes with a reduced surface electric field requirement thus lowering the Schottky correction peak ΔA values move to lower temperatures and smaller amplitudes. There is a discernible downward trend for the ionization layer voltage U_i, which stands for the potential drop across the area that accelerates ions toward the cathode, as the concentration of Sc increases. Under pure xenon conditions, U_i drops from 3.4 V at T_W = 3000 K to 2.7 V at T_W = 4000 K at 13 V. It dips further to about 2.1 V with Sc 5% and reaches 2.4 V with Sc 0.1%. At 25 V, a comparable trend is observed, with the initial U_i beginning at about 2.7 V and staying lower in the presence of Sc over the whole temperature range. The decrease in U_i is due to the increased ion density near the cathode due to effective ionization, reducing the potential energy needed for ion production and speeding up ions to maintain charge balance with thermionically released electron current. This enhanced plasma conductivity reduces overall voltage loss in this area as shown in Table 1.

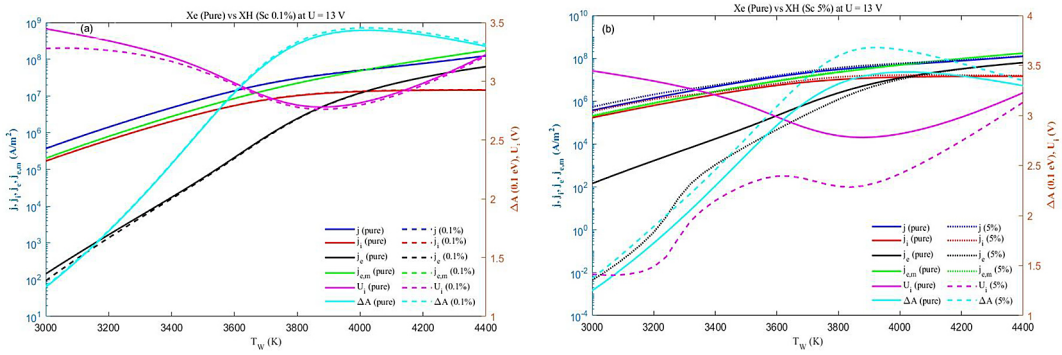

Figure 5. The density of the electric current components vs the surface temperature for 13 V Sc 0.1%, (b) Sc 5%

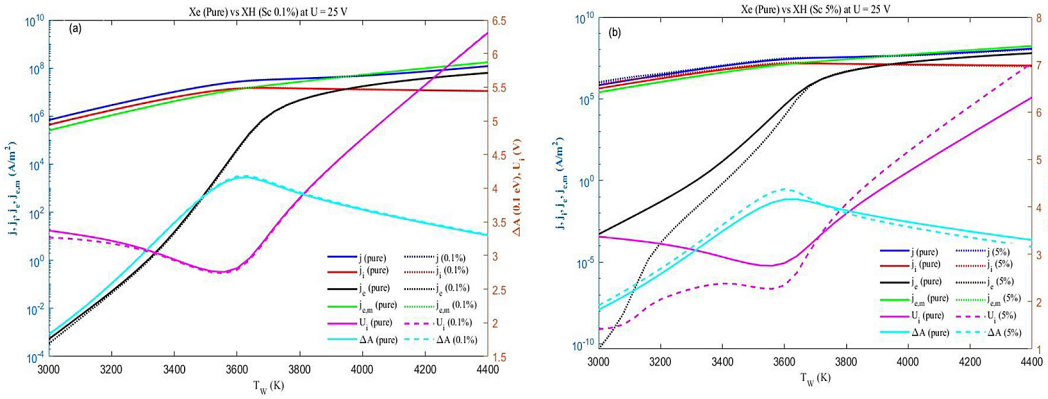

Figure 6. The density of the electric current components vs surface temperature for 25 V (a) Sc 0.1%, (b) Sc 5%

Table 1. Numerical values of ΔA peak and minimum U_i for different Sc concentrations and voltages

Gas / Sc content	Arc voltage (V)	T_w at ΔA peak (K)	ΔA peak (eV)	Minimum U_i (V)
Pure Xe	13	3900	3.4	2.7
0.1% Sc	13	3700	3.2	2.4
5% Sc	13	3600	3.0	2.1
Pure Xe	25	3700	5.5	2.7
0.1% Sc	25	3500	5.0	2.4
5% Sc	25	3400	4.3	2.1

CONCLUSIONS

The study found that a lower concentration of Sc 0.1% had minimal impact on plasma properties, suggesting that higher concentrations are needed to achieve performance improvements. Controlling Sc concentration, operating voltage, and cathode temperature can lead to more efficient plasma systems. The addition of ScI at a 5% concentration in xenon plasma increases total energy flux by 30%, maintaining high levels even at elevated temperatures. This is due to scandium's enhancement of plasma conductivity and its role in reducing thermal energy losses. Ion energy also increases by approximately 20%, and electron energy rises due to additional pathways for electron acceleration. The degree of ionization reaches 95% at 4000 K, demonstrating that Sc doping not only improves energy transport but also accelerates the transition to fully ionized plasma states.

Sc improves ionization and plasma conductivity in xenon plasma, reducing ΔA and U_i due to a lower electric field at the cathode surface and ion acceleration voltage in the ionization layer, and improving total cathode efficiency.

The study found that Sc, along with the potential difference, plays a significant role in influencing plasma parameters and stability, which is useful in practical applications of arc discharge plasma, especially in advancing the light lamp industry. Future studies should explore xenon plasma behavior with scandium additives under different discharge modes to understand transition mechanisms, surface interactions, and optimal operating conditions for enhanced stability and energy efficiency.

Acknowledgements

Authors would like to thank Mustansiriyah University (www.uomustansiriyah.edu.iq) Baghdad-Iraq for its support in the present work.

REFERENCES

1. Cunha, M. D., et al. Numerical and experimental investigation of thermal regimes of thermionic cathodes of arc plasma torches. *Journal of Physics D: Applied Physics* 2023; 56(39): 395204.
2. Jassam, H. F., and Ali, R. A. Interaction of near-cathode plasma layers with thermionic electrodes under high pressure arc plasma. *Journal of Physics: Conference Series*. 2022; 2322(1). IOP Publishing,
3. Santos, D. F. N., et al. Model of non-equilibrium near-cathode plasma layers for simulation of ignition of high-pressure arcs on cold refractory cathodes. *Journal of Physics D: Applied Physics* 2024; 57(40): 405202.
4. Zhou, W., et al. Particle-in-cell and Monte Carlo collision simulations of the cathode sheath in an atmospheric direct-current arc discharge. *Plasma Sources Science and Technology* 2016; 25(5): 05LT01.
5. Benilov, M. S. Nonlinear surface heating of a plane sample and modes of current transfer to hot arc cathodes. *Physical review E* 1998; 58(5): 6480.
6. Chemartin, L., et al. Modelling and simulation of unsteady dc electric arcs and their interactions with electrodes. *Journal of Physics D: Applied Physics* 2011; 44(19): 194003.
7. Villarreal-Medina, R., et al. Heat transfer mechanisms in arcs of various gases at atmospheric pressure. *Plasma Chemistry and Plasma Processing* 2023; 43(4): 787–803.
8. Li, He-Ping, and Benilov, M. S. Effect of a near-cathode sheath on heat transfer in high-pressure arc plasmas. *Journal of Physics D: Applied Physics* 2007; 40(7): 2010.
9. Zhukovskii, R., et al. Effect of cathode-plasma coupling on plasma torch operation predicted by a 3D two-temperature electric arc model. *Journal of Thermal Spray Technology* 2023; 32(2): 532–547.
10. Baeva, M., et al. Unified modelling of low-current short-length arcs between copper electrodes. *Journal of Physics D: Applied Physics* 2020; 54(2): 025203.
11. Mohsni, C., et al. Modelling and experimental investigations of DC electric arcs in argon and carbone dioxide. *Plasma Physics and Technology* 2019; 6(1): 51–55.

12. Lowke, John J., Anthony B. Murphy, and Manabu T. Cathode spot formation possibly explained by cathode electron emission from impact of excited state atoms. *Journal of Physics D: Applied Physics* 2019; 52(44): 444004.
13. Santos, D. F. N., et al. Numerical investigation of AC arc ignition on cold electrodes in atmospheric-pressure argon. *Journal of Physics D: Applied Physics* 2021; 54(19): 195202.
14. Mohsni, C., et al. Effect of a bidirectional coupling of an LTE arc column to a refractory cathode in atmospheric pressure argon. *Physics of Plasmas* 2020; 27(7).
15. Mohamed, Z. M., and Ali, R. A. Using Schottky Arc-plasma for modelling the cathode temperatures of various materials at high pressure. *Iraqi Journal of Science* 2024; 5037–5045.
16. Saber, T. A., Ali, R. A. and Jawad H. M. The role of cathode heat in the schottky correction in the ionization layers of arc plasma. *Advances in Science and Technology. Research Journal* 2024; 18(4).
17. Cunha, M. D., et al. Simulating changes in shape of thermionic cathodes during operation of high-pressure arc discharges." *Journal of Physics D: Applied Physics* 2019; 52(50): 504004.
18. Benilov, M. S. Understanding and modelling plasma–electrode interaction in high-pressure arc discharges: a review. *Journal of Physics D: Applied Physics* 2008; 41(14): 144001.
19. Benilov, M. S., and Cunha, M. D. Heating of refractory cathodes by high-pressure arc plasmas: II." *Journal of Physics D: Applied Physics* 2003; 36(6): 603.
20. Beilis, I. Theoretical modeling of cathode spot phenomena. *Handbook of vacuum arc science and technology*. William Andrew Publishing, 1996; 208–256.
21. Javidi-Shirvan, A. *Modelling of Cathode-Plasma Interaction in Short High-Intensity Electric Arc–Application to Gas Tungsten Arc Welding*. Chalmers Tekniska Hogskola (Sweden), 2016.
22. Benilov M.S. and Cunha M.D. Heating of refractory cathodes by high-pressure arc plasmas: II. J. Phys. D. Appl. Phys. 2003; 36(6): 603.
23. Almeida P.G.C., Benilov M.S., Cunha M.D. Formation of stationary and transient spots on thermionic cathodes and its prevention, J. Phys. D. Appl. Phys. 2008; 41(14), 144004
24. Krivtsun, I. V., Demchenko, V. F. and Krikent, I. V. Model of the processes of heat, mass and charge transfer in the anode region and column of the welding arc with refractory cathode. *The Paton Welding J* 2010; 6: 2–9.
25. Beilis, I. Theoretical modeling of cathode spot phenomena. *Handbook of vacuum arc science and technology*. William Andrew Publishing, 1996; 208–256.
26. Cao, S., et al. Modeling on plasma energy balance and transfer in a hollow cathode. *Journal of Physics D: Applied Physics* 2019; 52(28): 285202.
27. Benilov, M. S., and Marotta, A. A model of the cathode region of atmospheric pressure arcs. Journal of Physics D: Applied Physics 1995; 28(9): 1869.
28. Subramaniam, V. V., Hoyer K. S., and Lawless, J. L. Limits on steady diffuse mode operation of the cathode in magnetoplasmadynamic thrusters. Journal of Propulsion and Power 1991; 7(4): 565–572.